JAERI-M
4520

$^{208}Pb(\gamma, n)^{207}Pb$ Reaction near Threshold

July 1971

M. Mizumoto • Y. Nakajima • R. Bergère

T. Fuketa

日本原子力研究所
Japan Atomic Energy Research Institute

$^{208}Pb(\gamma,n)^{207}Pb$ Reaction near Threshold

M.Mizumoto, Y.Nakajima, R.Bergère* and T.Fuketa
Div. of Physics, Tokai, JAERI

(Received July 1971)

Abstract The photoneutron cross section for ^{208}Pb has been studied in several hundred keV region of neutron energy by the neutron time-of-flight technique. Spins and parities of the compound levels were determined by measuring the angular distribution of emitted neutrons, and the ratios of reaction matrix elements for channel spin 1 and 0 were calculated for the excited states of 1^+ of ^{208}Pb.

---

* Visiting scientist from C.E.N. de Saclay. Now at Departement de Physique Nucléaire / MF, C.E.N. de Saclay, France.

中性子分離エネルギー近傍における^{208}Pb（γ, n）反応

日本原子力研究所東海研究所物理部
水本元治
中島豊
更田豊治郎
R. Bergère*

（１９７１年７月受理）

要旨　原研リニアックの制動輻射線とラジオジェニックな^{208}Pb試料とを用いて，しきい値近傍の^{208}Pb（γ, n）反応からの中性子エネルギースペクトルを入射輻射線に対して８５度および１３０度の２方向について飛行時間法によって測定した。

１００KeVから７００KeVまでの放出エネルギー範囲において１０個の共鳴を観測し，数個の^{208}Pb複合核準位のスピン・パリティを決定した。特に1^+準位については反応のチャンネルスピン１および０に対する反応行列要素の比を求め，他の実験値と比較した。

＊　フランス　サクレー研究所

目　次　な　し

Introduction

Studies of neutron resonance levels by means of photoneutron reaction continue to give important informations to the nuclear physics. Energy spectrum of neutrons emitted from highly excited states of nuclei can be measured with good resolution by the time-of-flight technique. The basic idea of the measurement in this paper is illustrated in Fig. 1. It was originally applied by W.Bertozzi et al.[1] in their measurements on Pb and Bi, and it has been fully utilized by C.D.Bowman et al.[2)~6)] in their measurements on several nuclides. Bremsstrahlung beam produced by an electron linear accelerator excites nuclear states of a target nucleus. The tip of the bremsstrahlung spectrum is adjusted to exceed barely the neutron binding energy for the target nucleus, so that only the neutron emission to the ground state of the residual nucleus is energetically possible. The energy interval between the first excited state and the ground state of the residual nucleus is required to be not too narrow as compared with the accuracy of the tip energy of bremsstrahlung in order to confirm the above condition. The orbital angular momentum of emitted neutrons can be obtained by measuring the angular distribution of neutrons. Hence, spin and parity of the excited level are determined from the conservation of the angular momentum and the parity. Futhermore, the ground state radiation width, the neutron width and the level spacing will be obtained if the measurement is made with necessary accuracy. These information make a contribution to the study of the statistical property of the nucleus which the neutron spectroscopy is also concerned with. In the present work, the radiogenic ^{208}Pb isotope was chosen as the sample. The measurements on ^{208}Pb have been previously undertaken at other laboratories[1),4)]. The present experiment was planned to improve the data and to find more resonance levels than in the available data at that time, but recently Bowman et al.[6)] measured this nucleus with considerably high resolution. In the following, the results of measurements of the photoneutrons at two angles, 85° and 130° to the incident photons, and of the several spin-parity assignments of the levels are reported. For the 1^+ states of ^{208}Pb, the ratios of reactions matrix elements for channel spin 1 and 0 are discussed.

Experiment

The experiment was performed by using the neutron time-of-flight spectrometer at the JAERI linear accelerator. The experimental arrangement is shown in Fig.2. A detailed description of the instrumentation can be found in Ref. 7 except for the bremsstrahlung- and (γ,n)-target assemblage. The electron beam from the linear accelerator was energy-analyzed with a bending magnet and allowed to bombard a 1 mm tantalum bremsstrahlung target. A 100 mm graphite block was placed after the target to stop the electron beam completely. The target current from the insulated tantalum plate was measured to monitor the beam intensity. Gamma-rays from the tantalum target irradiated the ^{208}Pb sample of which thickness, weight and isotopic abundance were 12.0 gr/cm^2, 440.2 gr and 91 % ^{208}Pb and 7 % ^{207}Pb, respectively. Gamma-rays were incident upon the sample at 130° or 85° to the direction of the neutron detector on the neutron flight path, and distances from the sample to the neutron detector were 50.57 m and 49.80 m, respectively. The neutron flight path consisted of three evacuated tubes each with aluminum windows. In the flight path, a 10 mm natural uranium plate was inserted to reduce the gamma flash and a 3 mm boral plate to prevent the overlap of slow neutrons.

The neutron detector consisted of four sets of a ^6Li glass scintillator of $4\frac{3}{8}$ " dia.$\times\frac{1}{2}$ " thickness (NE905 or NE908 of Nuclear Enterprise) and a 5 " dia. photomultiplier of EMI-9579B. The signals from the photomultiplier were amplified and stored in a multichannel time analyzer. The channel width of the time analyzer was set at 62.5 nsec. The measurement was carried out with the electron beam energy of 10.5 MeV, the pulse repetition rate of 300 pps and the pulse width of 150 nsec. The peak electron beam current at the bremsstrahlung target was about 20 mA which was much lower than the value at the normal operating energy of 20 MeV. Though the electron beam energy of 10.5 MeV exceeded several excited levels of the residual nucleus, it was chosen to increase the bremsstrahlung intensity effective to excite the resonance levels of interest. The detection of neutrons to lead the first and the higher excited states of the residual nucleus was roughly checked preliminary, and was estimated to be negligible at the above condition.

Detector efficiency

It is important that the energy dependence of the neutron detector efficiency is accurately known, because the cross section value deduced from the yield is inversely proportional to the detector efficiency. It was determined in the following manner. A neutron generating target assemblage, which had a paraffin block moderator (20X30X10 cm^3) at the sample position, was bombarded by 18 MeV electron beam, so that relatively intense neutron flux of continuous energy spectrum was produced. A measured spectrum of this neutron beam by the ^6Li-glass detector is shown in Fig. 3. The figure represents the overall effect of the detector efficiency and the transmission of the aluminum, the uranium and the boral plates in the flight path. It was assumed that the neutron flux had a 1/E spectrum at the paraffin moderator of the target assemblage. One difficulty in the efficiency calculation was to determine the background in the spectrum of Fig. 3, and it was assumed to be constant and 400 counts/channel from the dip at 161 keV aluminum resonance which resulted from the relatively thick aluminum windows of the flight tubes and the aluminum case of the detector. The energy scale of the spectrum of Fig. 3 was also calibrated by the 161 keV aluminum dip. In the calculation of the relative cross section from the raw data, the energy scale of the efficiency curve was adjusted for a slight difference of the flight path length.

In order to check propriety of the above procedure, a spectrum which should be equivalent to that of Fig. 3 was constructed by the following calculation. In the calculation, 1) the efficiency of ^6Li glass detector was assumed to be $1 - e^{-N\sigma_{n,\alpha}}$ where $\sigma_{n,\alpha}$ was the (n,α) cross section of ^6Li and N the thickness of ^6Li in the glass; 2) density and thickness of the glass, and percentage of ^6Li in the glass were taken to be 2.48 gr/cm^3, 12.5 mm and 6.6 %, respectively; 3) the neutron source spectrum was assumed to have 1/E dependence; 4) materials in the neutron beam was assumed to be 13.4 mm of aluminum, 3 mm of boron and 10 mm of uranium; and 5) the cross section values were taken from BNL-325[8]. The spectrum obtained by this calculation is shown in Fig. 4 and it agrees qualitatively with that of Fig. 3.

Results and Discussion

The raw data at 130° and 85° are shown in Figs. 5 and 6. Relative cross sections which are deduced from the raw data are plotted in Figs. 7 and 8. Scatterings of the points in the lower energy region of the plots resulted from inaccurate structure in the efficiency curve due to the low efficiency and the poor statistics. The error bar in the figures represents a combined error of counting statistics and 10 % error in the sample thickness, but it does not include errors in the angle and the efficiency. The error of efficiency is, however, taken into account in the calculation of the area under the resonance peak. The resonance energies and peak areas are listed in Table 1 together with the data by Bowman et al.[6] to which the present values of the table are normalized at 257 keV resonance. In the calculation of the areas, the backgrounds are taken to be constant and to be 195 counts/channel for the data shown in Fig. 5 ($\theta_{\gamma,n}$=130°) and 92 counts/channel for the data shown in Fig. 6 ($\theta_{\gamma,n}$ = 85°). A considerable ambiguity in the peak area arised from the uncertainty of the detector efficiency. Three kinds of background, 350, 400 and 450 counts/channel, were assumed for the data shown in Fig. 3 and the scale of the time channel of the efficiency curve was shifted back and forth by one channel, then, with 9 different efficiency curves obtained in that manner, the areas were calculated in order to estimate the error component due to the uncertainty of the efficiency. The errors in Table 1 are combined ones of the above and the statistical errors of the counts. However the error of the standard, that is, the error of the area at the 257 keV resonance by Bowman et al., is not taken into consideration. In order to deduce the spin-parity of the each resonance level, the ratios between the areas at 85° and 130°, Area(85°)/Area(130°), were calculated and listed in Table 2. In this calculation, the ratios from the raw data instead of the cross section data were used to eliminate the ambiguity due to that of the detector efficiency. The ratios were also normalized at 257 keV, 1^- state[6]. The theoretical ratios of areas were calculated in accordance with the usual formula[9] for 1^-, 2^+ and 1^+ states of the excited nucleus, and are listed in Table 3 with the multipolarity of the radiations, the orbital angular momentum

and the channel spin. The error of the ratio is taken to be the mean square root of the statistical errors of the two areas. Although the angles are slightly different from each other, our data agree fairly well with those of Bowman et al. within the experimental errors and almost the same spin-parity assignments are claimed as those of Bowman et al. They utilized high resolution neutron total cross section data on ^{207}Pb from Duke University[10] as additional information on the parity assignment. We might not be able to claim the individual assignment of spin-parity in the table strongly from the quality of our data, but our results generally support the large M1 strength claimed by Bowman et al. Because the state 1^+ can have two channel spins, 1 and 0, the ratio of reaction matrix elements, (m_1/m_0), was calculated for the resonances assigned to be 1^+ or to have any possibility of being 1^+ from the following formula.

$$\text{Ratio of the areas} = \frac{(1-P_2(\cos\theta_1)) + \frac{m_1}{m_0}(1+\frac{1}{2}P_2(\cos\theta_1))}{(1-P_2(\cos\theta_2)) + \frac{m_1}{m_0}(1+\frac{1}{2}P_2(\cos\theta_2))}$$

where P_2 is the Legendre function of second order. These values are listed in Table 4. As far as the 1^+ assignment is correct, the (m_1/m_0) values in the columns II and III should be equal to each other for the same resonance. But, the values in the columns II and III do not agree with each other within the error at 182 keV and 615 keV resonances. The (m_1/m_0) values scatter largely among the resonances, although the errors are also quite large. We can not discuss the values in the table further because of those errors. However, we should point out the followings. The (m_1/m_0) values are quite sensitive for a discrepancy between the different experiments rather than the ratios of the resonance areas. In order to obtain (m_1/m_0) values with reasonable accuracy, the measurement with much higher accuracy than so far achieved and with one more detection angle is requested.

The present experiment was cut off to a certain extent by a reconstruction schedule of JAERI linac. The linac was shut down in March, 1970, and the new linac will be a 120 MeV machine in operation in 1972. A kind of experiment requested in the above will not be made by us in near future because of the high normal operating energy of the linac.

Acknowledgements

The authors wish to thank Dr. H. Takekoshi for his interest and support to this work. They are indebted to C.E.N. de Saclay for borrowing the radiogenic ^{208}Pb sample. They would like to express their gratitude to Dr. K . Harada for valuable suggestion and discussion, and to the operating staff of the Linac Laboratory for a hard operation of the linac near the end of its life and at a low beam energy which is out of the normal operating condition.

References

(1) W. BERTOZZI, C.P.SARGENT and W.TURCHINETZ : Phys. Letters 6 (1963) 108.

(2) C.D.BOWMAN, G.S.SIDHU and B.L.BERMAN ; Phys. Rev. 163 (1967) 951.

(3) B.L.BERMAN, R.L.VAN HEMERT and C.D.BOWMAN ; Phys. Rev. 163 (1967) 958.

(4) C.D.BOWMAN, B.L.BERMAN and H.E.JACKSON ; Phys. Rev. 178 (1969) 1827.

(5) C.D.BOWMAN, R.J.BAGLAN, B.L.BERMAN and T.W.PHILLIPS ; Phys. Rev. Letters 25 (1970) 1302.

(6) R.J.BAGLAN, C.D.BOWMAN and B.L.BERMAN ; Phys. Rev. C3 (1971) 672.

(7) A.ASAMI, T.FUKETA, Y.KAWARASAKI et al. ; JAERI 1138 (1967).

(8) M.D.GOLDBERG ; BNL-325 Second Edition Supplement No. 2 (1964～66).

(9) A.M.BALDIN, V.I.GOL'DANSKII and I.L.ROZENTHAL ; "Kinematics of Nuclear Reactions" Pergamon Press, New York,(1961).

(10) E.G.BILPUCH ; private communication (1969) in Ref. 6.

Table 1. ^{208}Pb (γ,n) Resonance energies and areas

Label of peak	Present data					Bowman et al.[6] +		
		$\theta_{\gamma n}$ = 85°		$\theta_{\gamma n}$ = 130°				
	Energy (keV)	Area (arbitrary unit)	$\frac{A}{\lambda^2}$ (eV)	Area (arbitrary unit)	$\frac{A}{\lambda^2}$ (eV)	Energy (keV)	$\frac{4\pi A}{2\pi^2 \lambda^2}$ (eV)	ES++ or GS
J	116	$0.6^{+0.3}_{-0.2}$	$1.2^{+0.5}_{-0.4}$	$0.6^{+0.1}_{-0.1}$	$1.3^{+0.3}_{-0.3}$	114	2.0	
I	130	$1.3^{+0.6}_{-0.3}$	$2.4^{+1.1}_{-0.7}$	$1.0^{+0.1}_{-0.1}$	$2.1^{+0.3}_{-0.3}$	129	5.4	GS
						138	3.6	ES
						156	0.98	GS
H	168	$1.5^{+2.1}_{-0.9}$	$2.8^{+3.9}_{-1.7}$			166	0.90	GS
G	182	$15.3^{+6.2}_{-3.7}$	28^{+12}_{-7}	$10.5^{+3.6}_{-2.4}$	$22.5^{+7.7}_{-5.2}$	182	16.0	GS
F	257*	$13.9^{+2.0}_{-1.6}$	26.2*	$12.0^{+0.8}_{-0.7}$	26.2*	257	26.2	GS
E	301**	$2.3^{+1.2}_{-1.0}$	$4.4^{+2.3}_{-1.9}$	$1.7^{+0.2}_{-0.2}$	$3.8^{+0.4}_{-0.4}$	299	4.0	ES
D	317 (333)***	$6.1^{+2.1}_{-1.7}$	$11.7^{+4.0}_{-3.3}$	$5.2^{+0.4}_{-0.4}$	$11.5^{+0.9}_{-0.9}$	318	11.0	GS
C	430 (460)***	$8.2^{+4.4}_{-3.9}$	$16.1^{+8.7}_{-7.7}$	$5.4^{+0.9}_{-0.9}$	$12.2^{+2.0}_{-2.0}$			
						493	3.2	
B	546	$7.5^{+2.9}_{-2.3}$	$15.2^{+5.9}_{-4.7}$	$5.3^{+1.1}_{-1.0}$	$12.4^{+2.6}_{-2.3}$	547	12.3	GS
						558	4.6	
A	615	$12.1^{+4.9}_{-3.3}$	25^{+10}_{-7}	$8.7^{+2.6}_{-2.2}$	$20.7^{+6.2}_{-5.2}$	620	17.2	GS

+The data of Bowman et al. cover a broader energy region than that of this table.
++GS and ES indicate the ground state transition and the excited state transition, respectively.
* The resonance energies and peak areas are normalized at 257 keV resonance to the data by Bowman et al.
** ES peak assigned by Bowman et al. *** not well resolved peak.

Table 2. Ratio of areas and spin-parity assignment

label of peak	present date				Bowman et.al.[5),6)]	
	Area(85°) (counts)	Area(130°) (counts)	Ratio Area(85°) / Area(130°)	J^π	Ratio Area(90°) / Area(135°)	J^π
J	115 ± 35	105 ± 47	1.53 ± 0.83	1^+	1:54 ± 0.22	1^+
I	235 ± 42	260 ± 57	1.26 ± 0.36	$1^+(1^-)$		1^+ 2^{+*}
G	845 ± 45	985 ± 57	1.20 ± 0.10	1^+	1.45 ± 0.20	1^+
F	2790 ± 75	3890 ± 93	1	1^-	1	1^-
D	635 ± 52	890 ± 67	1.00 ± 0.12	1^+	1.13 ± 1.16	1^+
C	440 ± 59	665 ± 74	0.92 ± 0.16	1^- 1^+		
B	195 ± 41	355 ± 53	0.77 ± 0.20	$1^+(1^-)$	0.94 ± 0.13	$1^-(1^+)$
A	495 ± 49	515 ± 61	1.34 ± 0.21	1^+	1.81 ± 0.25	1^+

* This assignment was made in Ref. 5 but not seen in Ref. 6.

Table 3. The theoretical ratios between the areas at 85° and 130°

Multiporality of transition	J^{π} of resonance state	Angular momentum of emitted neutron	Channel spin	Theoretical value of area ratio*
E 1	1^-	S	0	1
M 1	1^+	P	1 , 0	0.635 ~ 2.402
M 2	2^+	P	1	0.635

* Area ratio is defined by Area (85°)/Area (130°).

Table 4. The ratio of reaction matrix elements between channel spins, 1 and 0, for the 1^+ state, $\left(\frac{m}{m}_{0}^{1}\right)$.

label of peak	Present data	Values calculated from Ref. 6
J	0.51 ± 0.67	0.35 ± 0.19
I	0.95 ± 0.62	
G	1.11 ± 0.22	0.47 ± 0.21
D	2.00 ± 0.68	1.25 ± 0.49
C	2.7 ± 1.5	
B	6.3 ± 9.4	2.6 ± 1.3
A	0.78 ± 0.28	0.11 ± 0.15

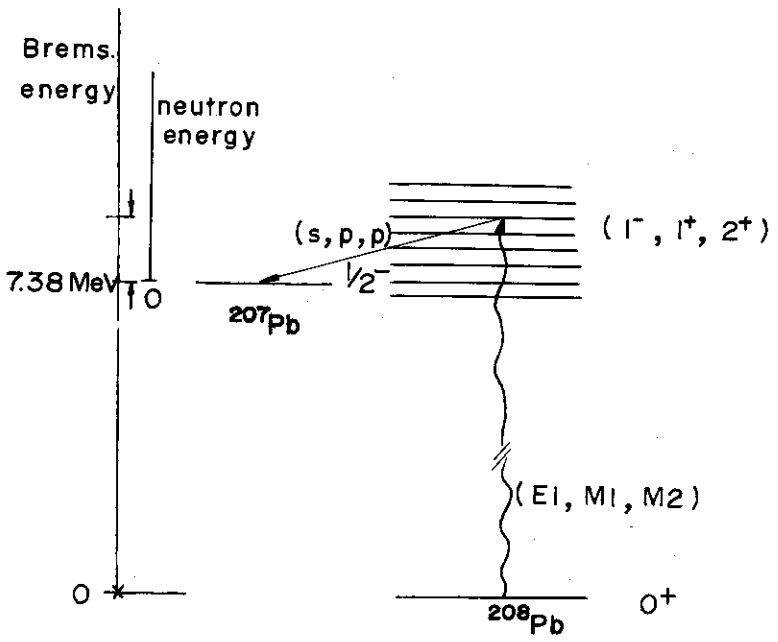

Fig. 1 Schematic representation of $^{208}Pb(\gamma,n)^{207}Pb$ reaction

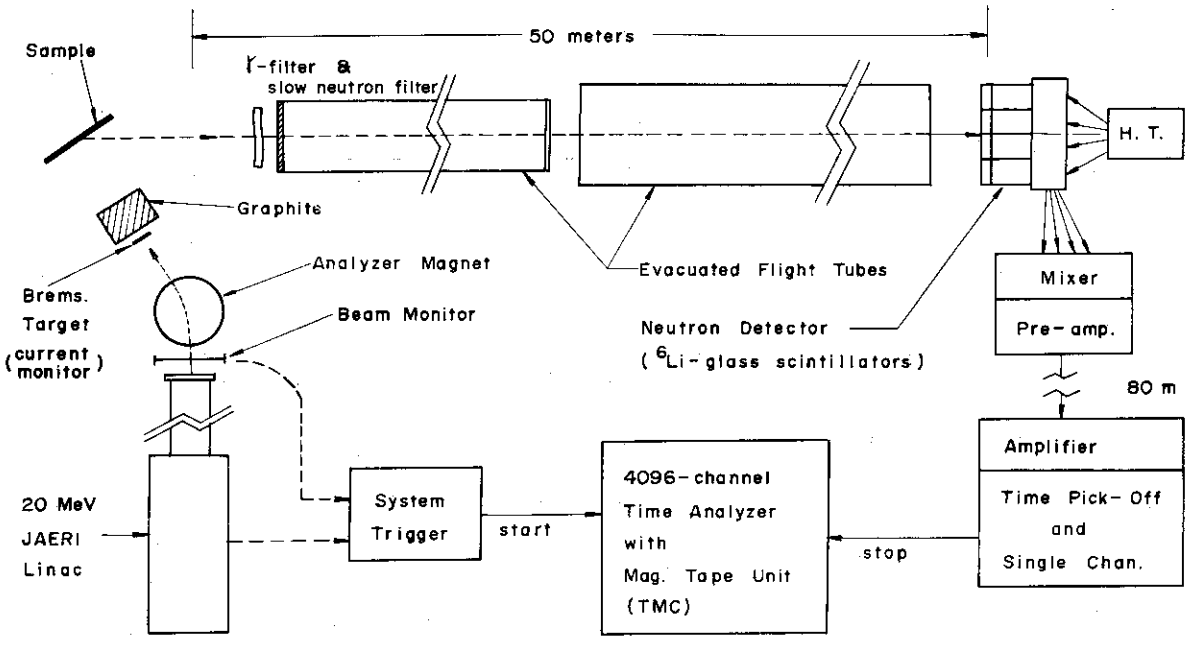

Schematic block diagram of the (γ,n) measurement

Fig. 2 Schematic block diagram of the (γ,n) measurement

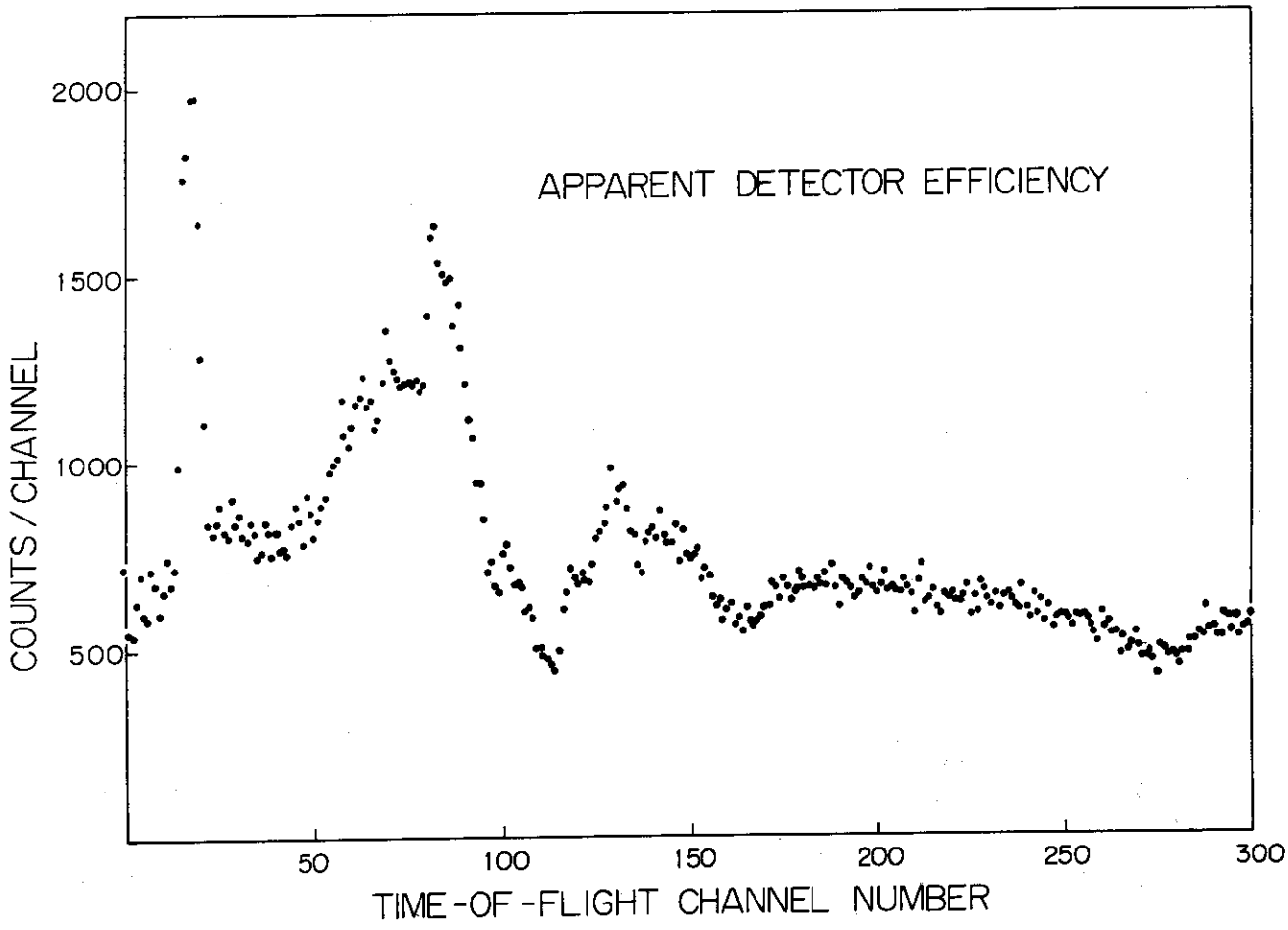

Fig. 3 The apparent detector efficiency obtained experimentally. This spectrum includes the convoluted effects of the efficiency of ^{6}Li glass detector, the spectrum of the neutron flux and the transmission of the materials in the flight path.

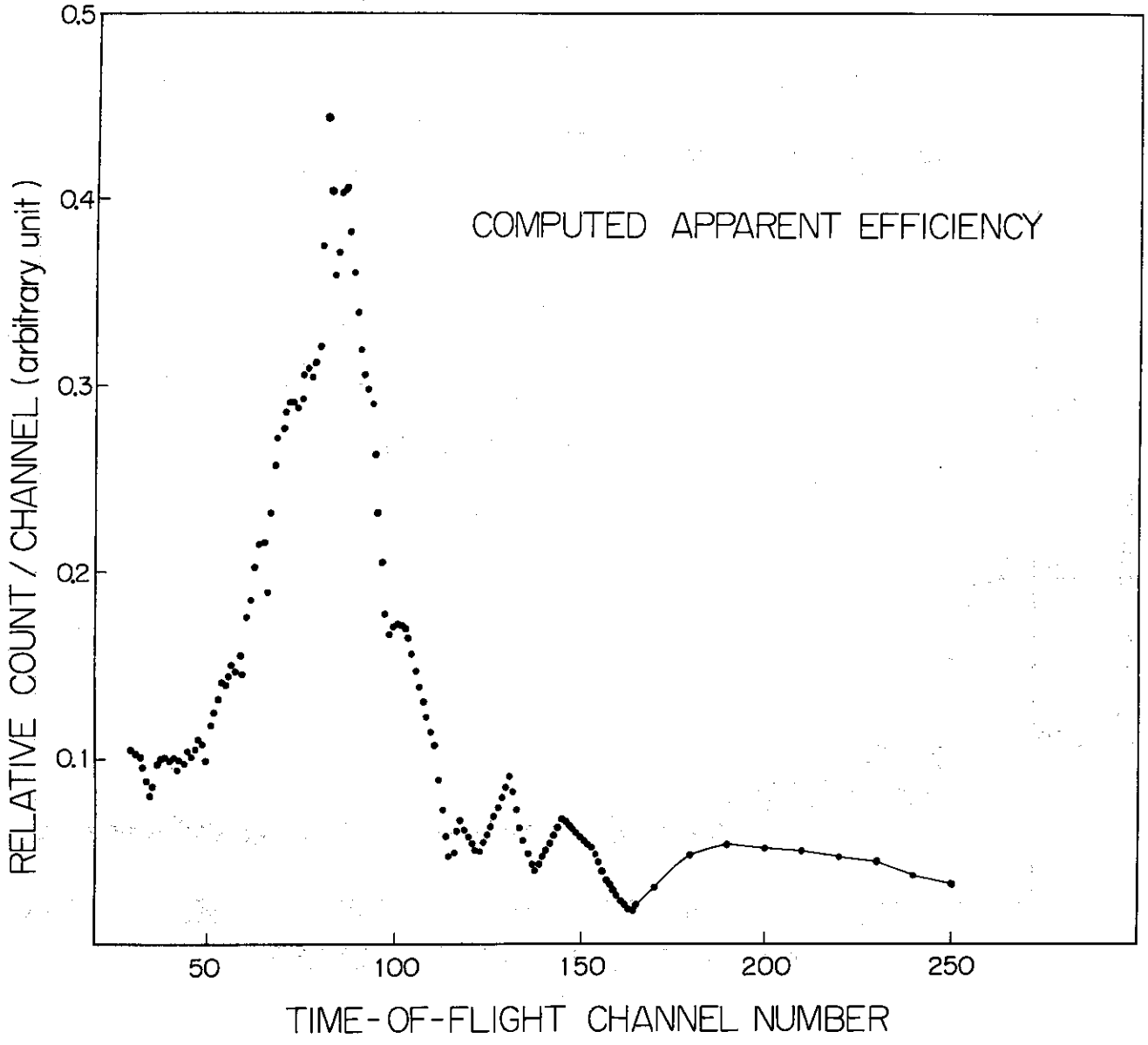

Fig. 4 The apparent detector efficiency computed by using the cross section values of BNL-325 in order to check the propriety of Fig. 3. This spectrum includes the convoluted effects of the efficiency of ^{6}Li glass detector the assumed spectrum of the neutron flux and the transmission of the material in the flight path.

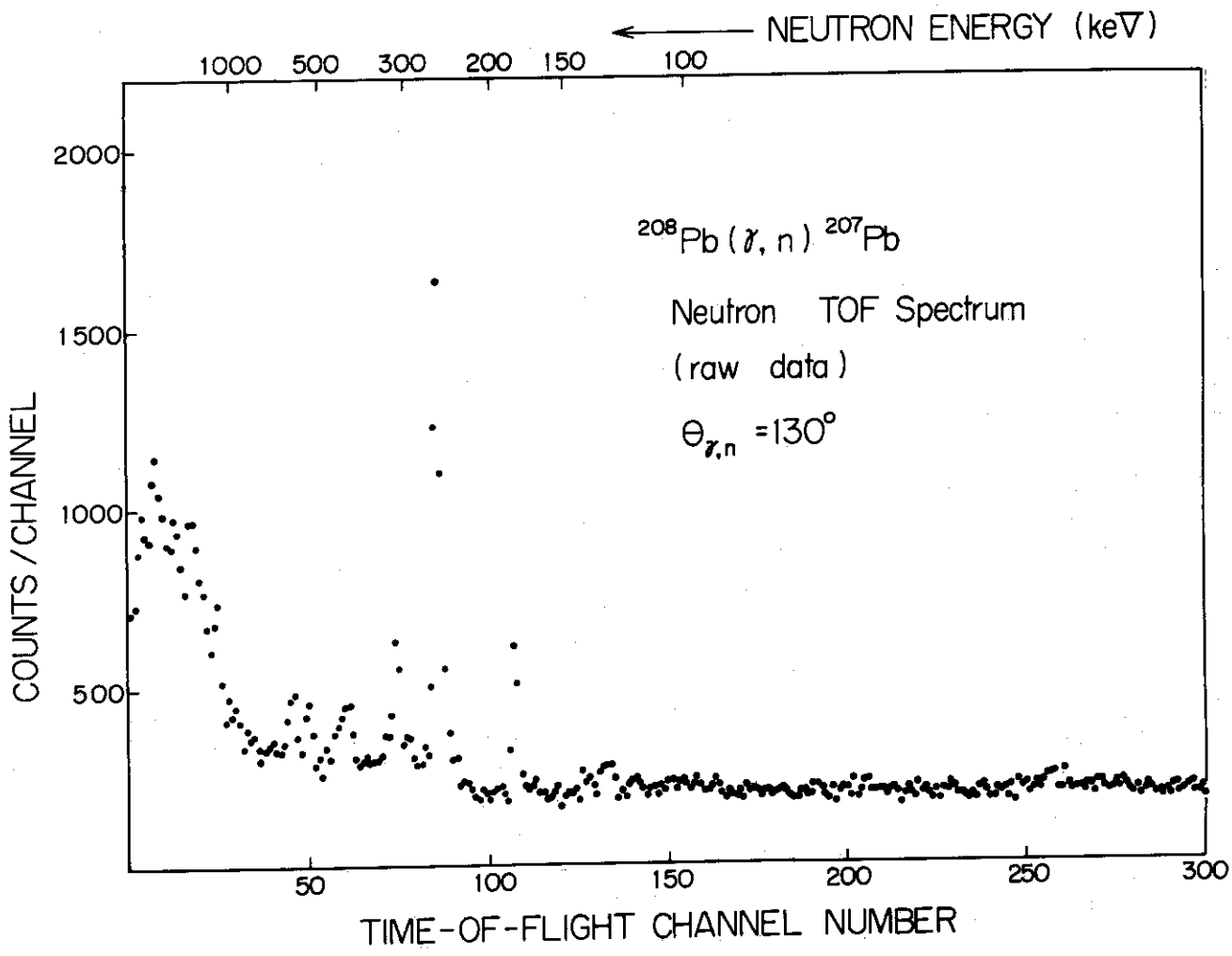

Fig. 5 Neutron time-of-flight spectrum (raw data) of $^{208}Pb(\gamma,n)^{207}Pb$ at 130°.

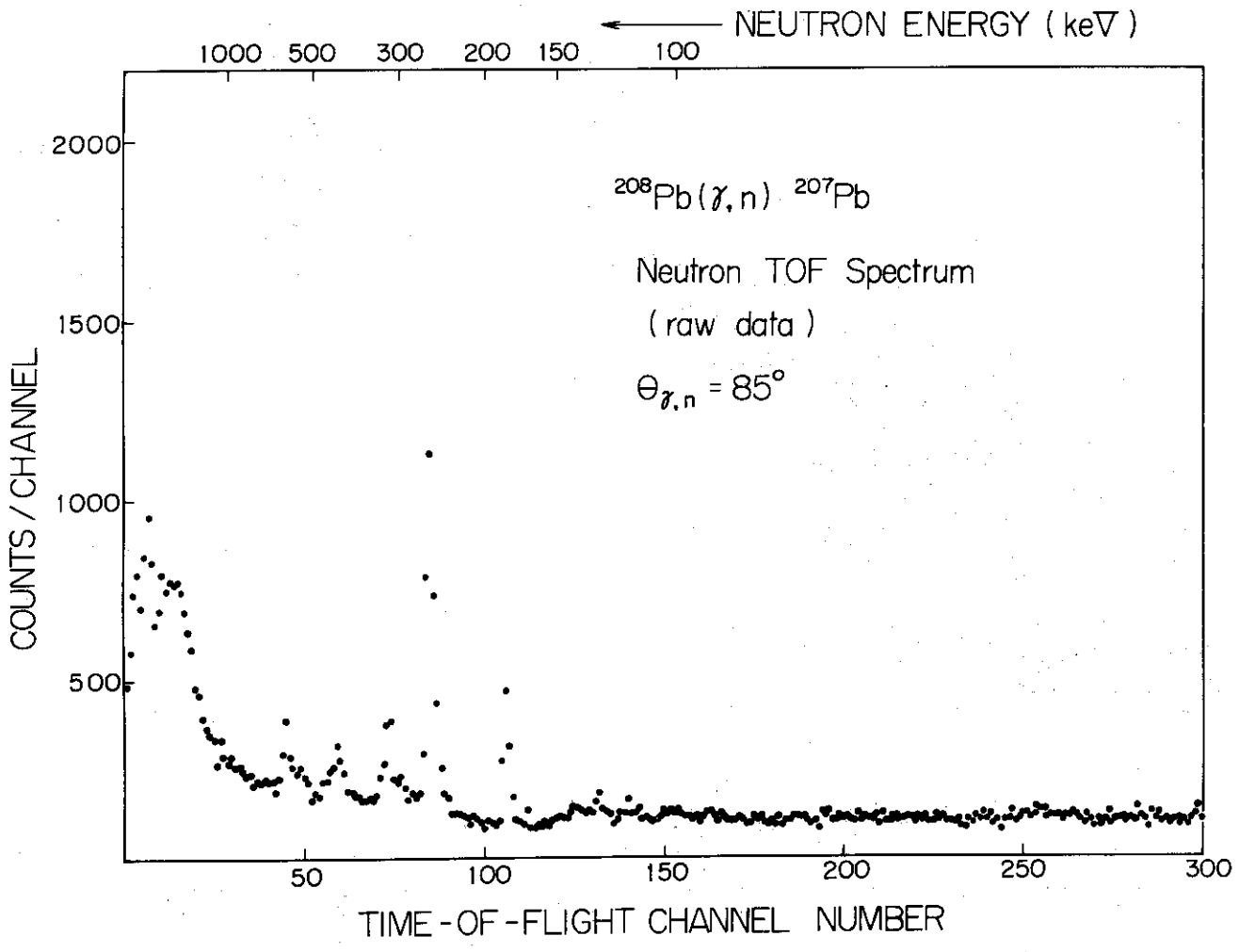

Fig. 6 Neutron time-of-flight spectrum (raw data) of $^{208}Pb(\gamma,n)^{207}Pb$ at 85°.

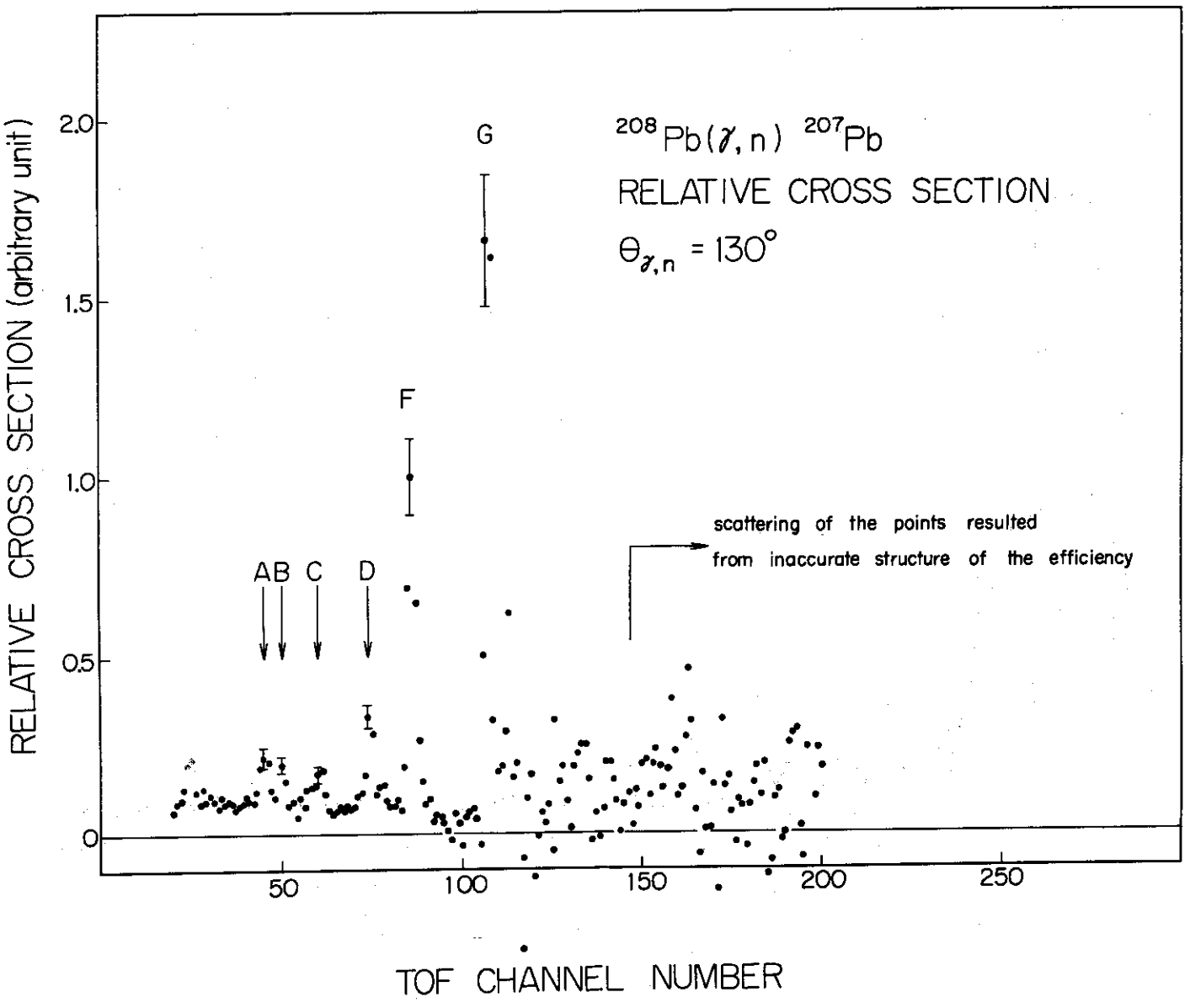

Fig. 7 Relative cross section of $^{208}Pb(\gamma,n)^{207}Pb$ at 130°.
Scattering of the points at the low energy region resulted from inaccurate structure of the efficiency. The error bar represents a combined error of counting statistics and 10 % error in the sample thickness.

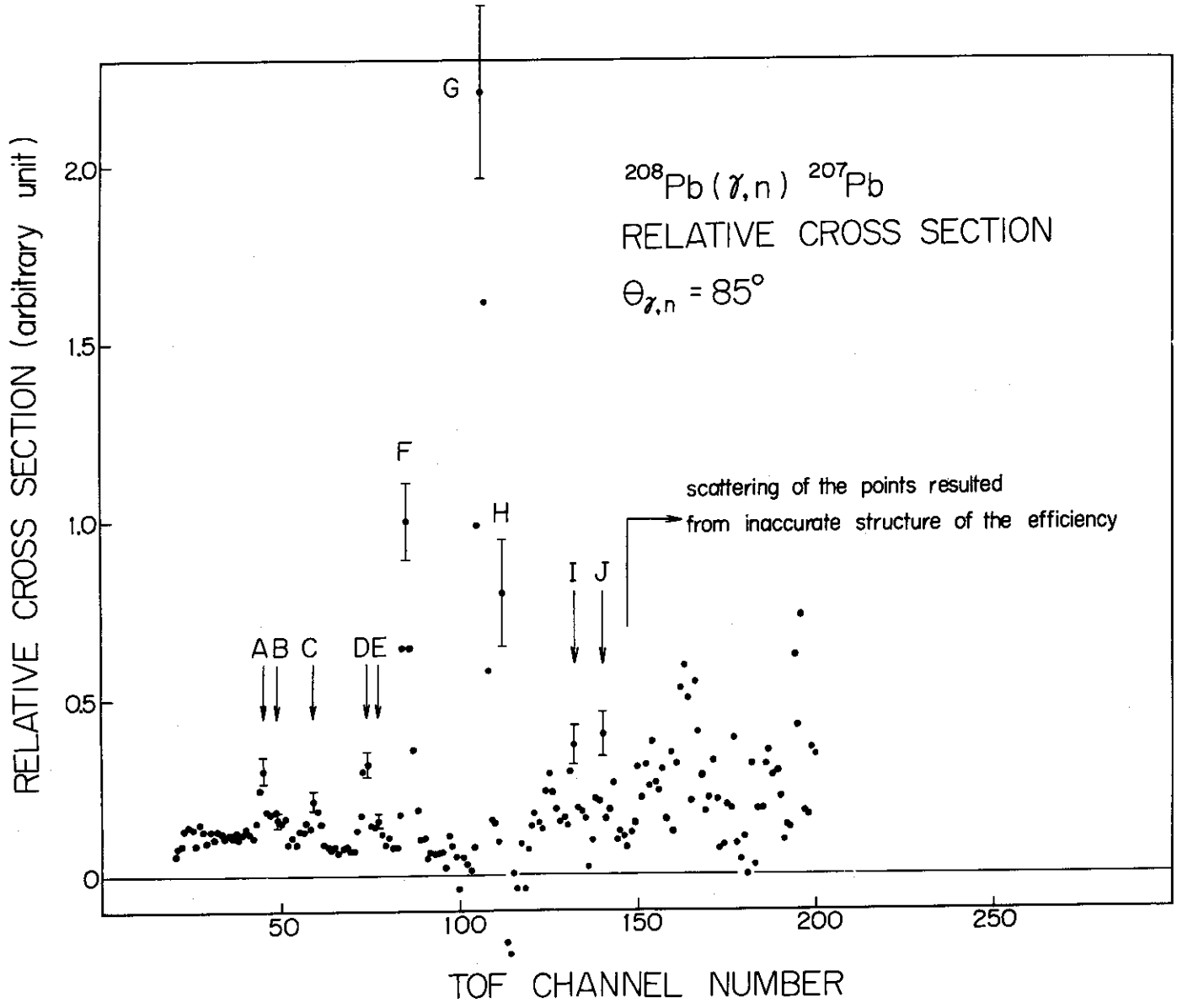

Fig. 8 Relative cross section of $^{208}Pb(\gamma,n)^{207}Pb$ at 85°.
Scattering of the points at the low energy region resulted from inaccurate structure of the efficiency. The error bar represents a combined error of counting statistics and 10 % error in the sample thickness.